Tellus (1981), *33*, 564–582

Deepening of the wind-mixed layer: A model of the vertical structure

By BENOÎT CUSHMAN-ROISIN[1], *Mesoscale Air-Sea Interaction Group, Florida State University, Tallahassee, Florida 32306 U.S.A.*

(Manuscript received December 22, 1980; in final form March 26, 1981)

ABSTRACT

A new non-linear model of mixing and convection based upon a modelling by two buoyant interacting fluids is applied to the deepening of the wind-mixed layer. In view of simple algebra, the model is one-dimensional, frictionless, and neglects the turbulence production by the mean-flow shear in the thermocline. The potential-energy increase required for deepening is thus supplied by the turbulence input at the surface (turbulent erosion model). A non-similar analytical solution is found in the case of a well-mixed layer bounded below by a sharp thermocline, treated as a boundary layer. This solution is valid if the frictional Richardson number, Ri, defined as the ratio of the total mixed-layer buoyancy to the friction-velocity squared, is much greater than unity. The model predicts an entrainment rate proportional to Ri^{-1}, and a ratio of thermocline thickness to mixed-layer depth of the order of $Ri^{-3/4}$. The thermocline shallows as $h^{-1/2}$, as the mixed-layer depth, h, increases with time. The vertical structure throughout the mixed layer and thermocline is given by the solution, and vertical profiles of mean values and vertical fluxes are plotted. These profiles are comparable to those obtained by turbulence-closure numerical models.

1. Introduction

Much of the work on upper ocean mixing is limited to one-dimensional models. These can be useful because bulk temperatures and salinities tend to vary more along a vertical distance of a hundred meters than along a horizontal distance of a thousand kilometers. This holds true over many parts of the world's oceans, except near fronts, because vertical exchange processes between the air and the sea, as well as vertical mixing within the water column, are likely to affect local conditions much more rapidly and effectively than horizontal advection and horizontal mixing (Niiler and Kraus, 1977).

Time-dependent one-dimensional models often assume vertical homogeneity in the mixed layer, and are therefore bulk models. They were reviewed extensively by Niiler and Kraus (1977), Kitaigorodskii (1979) and Zilitinkevich et al. (1979). The four unknowns in these models are the mixed-layer temperature $\overline{T}$, horizontal velocity components $\overline{u}$, $\overline{v}$, and thickness h. These variables are functions of time only and are governed by the overall budgets of heat, horizontal momentum and turbulent kinetic energy. This last budget takes the form:

$$\frac{d}{dt} TKE = F_s + E - \frac{d}{dt} PE - D - F_h \tag{1}$$

expressing that the time rate of change of the turbulent kinetic energy (TKE) is the sum of a surface flux F_s from the atmosphere through surface-wave breaking and the rate of production E by the shear of the mean flow minus the rate of increase of potential energy PE, the rate of dissipation D by friction within the mixed layer, and

[1] Present address: Department of Oceanography, WB-10, University of Washington, Seattle, WA 98195 U.S.A.

0040-2826/81/060563-19$02.50/0

the flux F_h of energy lost by internal gravity waves through the underlying stable layers.

It is reasonable to state that the turbulent kinetic energy responds quasi-instantaneously to time variations and thus to neglect its time rate of change (Denman, 1973; Niiler, 1975; Cushman-Roisin, 1981). On the other hand, the downward flux by internal gravity waves is often neglected since no acceptable parametrization has yet been proposed. The *TKE*-budget (1) therefore reduces to:

$$\frac{dPE}{dt} = F_s + E - D \tag{2}$$

which leads to two main classes of models: (i) *Turbulent erosion models* (TEM) for which the increase in potential energy by mixing is exclusively due to the surface flux F_s minus internal dissipation, and (ii) the *dynamic instability models* (DIM) for which the increase in potential energy is entirely due to production of turbulence by the mean-flow shear. The comparison and synthesis of these two models are discussed by Niiler (1975), de Szoeke and Rhines (1976) and Price et al. (1978).

More recently, various turbulence closure models have been applied to the mixed-layer deepening problem in order to study the vertical structure across the layer (Mellor and Durbin, 1975; Warn-Varnas and Piacsek, 1979; Klein, 1980; Kundu, 1980). They all show that the assumption of vertical homogeneity is excellent for temperature when the mixed layer is deep enough so that the thermocline is well-defined, but not adequate for horizontal velocity components for sub-inertial time scales when an Ekman-spiral structure is present.

In a parallel way, laboratory simulations of mixed-layer deepening were conducted, either without mean shear (oscillating-grid experiments by Turner and Kraus, 1967; Linden, 1975) or with mean shear (Kato and Phillips, 1969; Moore and Long, 1971; Kantha, Phillips and Azad, 1977).

Finally, theoretical and laboratory results have been compared with observations (Turner, 1969; Denman and Miyake, 1973; Halpern, 1974; Kullenberg, 1977; Price, Mooers and Van Leer, 1978; Dillon and Powell, 1979; Kitaigorodskii, 1979). The main conclusions resulting from the data are: (i) TEM and DIM both lead to qualitative agreement, (ii) good quantitative agreement is obtained for a well-adjusted dissipation term, and (iii) comparisons of the various terms in (2) favor a TEM if rotation is present and if the mixed layer is well-developed (i.e., after a few inertial periods).

2. The model

The model presented here is a new turbulent erosion model (TEM). It focuses on the vertical structure of the variables throughout the mixed layer and thermocline. The aim is to predict by simple analytical calculations the thermocline thickness and profiles of temperature, velocity, Reynolds stresses and heat flux. The model is based on a new parametrization of mixing and convection (Cushman-Roisin, 1981). It can be applied to the most general case of mixed-layer deepening under variable wind stress and/or variable surface heat flux.

The model envisions mixing as the relative motion of two interacting fluids of different properties. Parcels of fluid which have risen through the convective layer are given extra momentum by the wind stress near the surface, and their temperature is altered by the surface heat flux. These elements are pushed back into the convective layer by turbulence with new properties. Because they sink in a slightly stratified fluid, they accelerate or decelerate. Ultimately, they will become buoyant and decelerate. As they sink, they also progressively lose their horizontal-momentum excess and heat content by interactions with the upward return flow. As they reach the bottom, they have a null vertical velocity and lose their ability to carry heat and momentum. The active sinking elements are called *thermals*, and the rising elements *anti-thermals*, by analogy. The model describes the individual dynamics of thermals and anti-thermals, and their exchanges; mean properties and relative differences are then deduced. This permits direct computation of men profiles and vertical fluxes of momentum and heat.

For better comparison with previous models and laboratory experiments, the present study is limited to the case of no surface heat flux. This wind-mixed layer deepening case is depicted in Fig. 1. At the surface, non-buoyant thermals are produced by wind action. As they penetrate the *mixed layer*, they acquire positive buoyancy due to a slight stable stratification existing in that

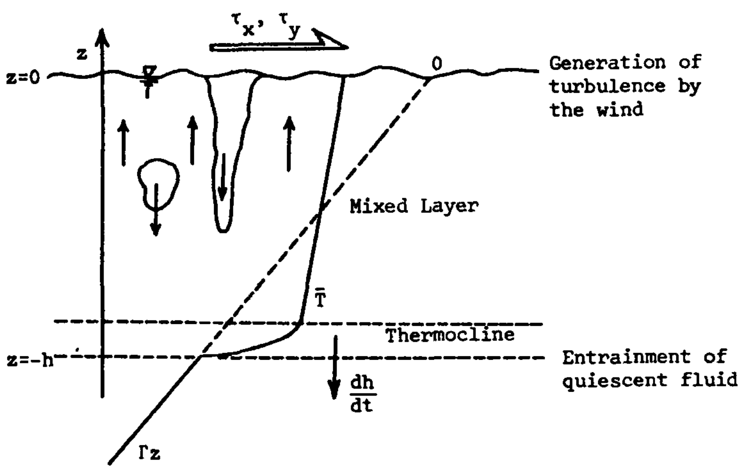

Fig. 1. Schematic model of the wind-mixed layer.

layer, and decelerate. At the bottom of the mixed layer, their vertical velocity is somewhat reduced. As the temperature profile begins to curve at the entrance of the thermocline, the thermals' buoyancy increases sharply, and their vertical velocity decreases rapidly. Since the newly entrained fluid is subjected there to the largest temperature variations, the vertical heat flux $\overline{wT}$ (negative) is large at the bottom of the mixed layer. A decreasing velocity therefore implies larger temperature contrasts and increasing buoyancy forces, which in turn decelerate thermals even more. The process is cumulative, and gives rise to the formation of a thin layer of rapid variations, the *thermocline*, which lies between the mixed layer and the quiescent stable fluid.

Throughout the mixed layer and thermocline, a saturation equilibrium between thermals and anti-thermals can be assumed (Cushman-Roisin, 1981). This leads to assigning a constant value to f, the fraction of area occupied by thermals. However, continuity of physical properties at the bottom of the thermocline requires f to vanish at that level. This may be accomplished by assuming the existence of an *entrainment layer* within which f decreases monotonically from its constant value in the mixed layer and thermocline to zero. Calculations carried out in Appendix A show that this layer is in fact so thin that it does not play any active role in the deepening process and may be neglected. It is therefore assumed here that f is constant throughout the water column.

3. Governing equations

Thermals and anti-thermals are characterized by different velocities, temperatures, densities and pressures. Primed and double-primed quantities refer to thermals and anti-thermals, respectively. If f represents the fraction of area occupied by thermals at any level, the fraction of area available to anti-thermals is $(1-f)$, so that mean properties are defined by:

Mean temperature

$$\bar{T} = fT' + (1-f)\,T'' \tag{3}$$

Mean velocity components

$$\bar{u} = fu' + (1-f)\,u'' \tag{4}$$

$$\bar{v} = fv' + (1-f)\,v'' \tag{5}$$

$$\bar{w} = fw' + (1-f)\,w'' \tag{6}$$

Mean density

$$\bar{\rho} = f\rho' + (1-f)\,\rho'' \tag{7}$$

Mean pressure

$$p = fp' + (1-f)p'' \tag{8}$$

Moreover, root-mean-square (rms) fluctuations are defined by:

$$a_{\text{rms}} = \sqrt{f(1-f)}(a' - a'') = \pm\overline{(a - \bar{a})^2}^{1/2} \tag{9}$$

where a stands for any physical quantity such as temperature, velocity, density or pressure. Rms fluctuations are thus proportional to the difference between thermals' and anti-thermals' quantities. They may be positive or negative. The vertical convective heat flux can be expressed as:

$$\overline{wT} = fw'T' + (1-f)w''T'' \\ = \overline{w}\overline{T} + w_{\rm rms}T_{\rm rms} \tag{10}$$

and all the other fluxes such as the Reynolds stresses can be written in similar forms:

$$-\overline{uw} = -\overline{u}\,\overline{w} - u_{\rm rms}w_{\rm rms} \tag{11}$$

$$-\overline{vw} = -\overline{v}\,\overline{w} - v_{\rm rms}w_{\rm rms} \tag{12}$$

$$-\overline{ww} = -\overline{w}^2 - w_{\rm rms}^2 \tag{13}$$

It is worth noting here that the concept of a two-fluid system leads to correlation coefficients equal to unity. This is coherent with Langmuir cell-type convection, which can have very high correlation coefficients (Thompson, 1981, private communication).

With these definitions and in the framework of the Boussinesq approximations, the one-dimensional inviscid convection (no horizontal variations, no dissipation) can be described by the following equations (Cushman-Roisin, 1981):

Continuity equation:

$$\overline{w} = 0 \tag{14}$$

Heat equations:

$$\frac{\partial \overline{T}}{\partial t} = -\frac{\partial}{\partial z}(w_{\rm rms}T_{\rm rms}) \tag{15}$$

$$\frac{\partial}{\partial z}(\overline{T} + mT_{\rm rms}) = 0 \tag{16}$$

Horizontal momentum equations:

$$\frac{\partial \overline{u}}{\partial t} - f_0\overline{v} = -\frac{\partial}{\partial z}(u_{\rm rms}w_{\rm rms}) \tag{17}$$

$$\frac{\partial \overline{v}}{\partial t} + f_0\overline{u} = -\frac{\partial}{\partial z}(v_{\rm rms}w_{\rm rms}) \tag{18}$$

$$\frac{\partial}{\partial z}(u + 2mu_{\rm rms}) = 0 \tag{19}$$

$$\frac{\partial}{\partial z}(\overline{v} + 2mv_{\rm rms}) = 0 \tag{20}$$

Vertical momentum equations:

$$\frac{1}{\rho_0}\frac{\partial \overline{p}}{\partial z} = -g[1 - \alpha(\overline{T} - T_0)] - \frac{\partial}{\partial z}w_{\rm rms}^2 \tag{21}$$

$$3mw_{\rm rms}\frac{\partial w_{\rm rms}}{\partial z} = \alpha g T_{\rm rms} - \frac{1}{\rho_0}\frac{\partial p_{\rm rms}}{\partial z} \tag{22}$$

Pressure fluctuation:

$$p_{\rm rms} = -\rho_0 m(u_{\rm rms}^2 + v_{\rm rms}^2) \tag{23}$$

Equation (14) is a result of the continuity for the mean flow and expresses that, in the absence of horizontal variations, the mean vertical velocity ought to be zero. Equations (15), (17) and (18) are the mean heat and horizontal-momentum budgets; they express that the time rates of change of mean temperature and horizontal velocity are equal to the divergences of the vertical fluxes of heat and horizontal momentum (convective heat flux and Reynolds stresses, respectively); f_0 is the Coriolis parameter equal to twice the angular rotation of the system. Equations (16), (19) and (20) result from the assumption that turbulent motions are at all times in quasi-equilibrium with their environment and express that mean and turbulent variables are correlated in a simple linear manner. The coefficient m is a function of f only and is defined by:

$$m = \frac{1-2f}{2\sqrt{f(1-f)}}. \tag{24}$$

Fig. 2 exhibits a plot of m versus f. Unlike eq. (16), eqs. (19) and (20) contain a factor two. The

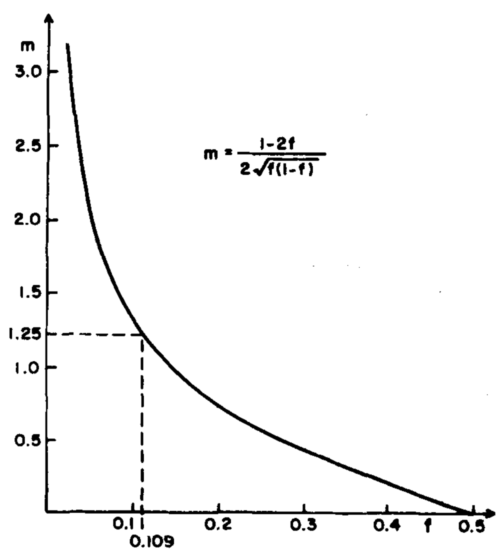

Fig. 2. Plot of m versus f, the fraction of area occupied by thermals.

presence of this factor results from the fact that the horizontal momentum equations contain a pressure term. Equation (21) is the hydrostatic balance modified by turbulent vertical motions; ρ_0 is the reference density at temperature T_0, and α is the coefficient of thermal expansion. Equation (22) is the vertical momentum equation after its mean has been subtracted; it expresses that thermals accelerate or decelerate due to their buoyancy or due to pressure fluctuations, which transfer turbulent kinetic energy between horizontal and vertical motions. The turbulent kinetic energy budget relates $p_{\rm rms}$ to $u_{\rm rms}$ and $v_{\rm rms}$, as expressed by (23).

Eliminating the equations for $\bar{w}$ and $\bar{p}$, (14) and (21), and replacing $p_{\rm rms}$ by its expression (23), the system reduces to seven non-linear first-order coupled differential equations.

4. Boundary conditions

At the surface, $z = 0$, the Reynolds stresses ought to match the wind-stress components:

$$-\overline{uw} = -u_{\rm rms}\, w_{\rm rms} = \frac{\tau_x}{\rho_0} \tag{25}$$

$$-\overline{vw} = -v_{\rm rms}\, w_{\rm rms} = \frac{\tau_y}{\rho_0} \tag{26}$$

while the vertical convective heat flux is set equal to zero:

$$\overline{wT} = w_{\rm rms}\, T_{\rm rms} = 0 \tag{27}$$

since the effect of a surface heat flux is not studied here. Finally, isotropic turbulence is assumed in the wave zone just beneath the surface:

$$w^2_{\rm rms} = u^2_{\rm rms} + v^2_{\rm rms} \tag{28}$$

expressing that the turbulent vertical velocity equals the turbulent horizontal velocity.

The wind-stress amplitude defines a friction velocity characteristic of the turbulence near the surface:

$$u_* = [(\tau_x/\rho_0)^2 + (\tau_y/\rho_0)^2]^{1/4} \tag{29}$$

In terms of this friction velocity, the surface boundary conditions (25), (26), (27) and (28) become:

$$\begin{aligned} u_{\rm rms} &= \tau_x/(\rho_0 u_*) \\ v_{\rm rms} &= \tau_y/(\rho_0 u_*) \end{aligned} \tag{30}$$

$$\begin{aligned} w_{\rm rms} &= -u_* \\ T_{\rm rms} &= 0 \end{aligned} \tag{31}$$

where $w_{\rm rms}$ is chosen to be negative because thermals sink ($w' < 0 < w''$).

At the bottom, $z = -h(t)$, mean quantities match the characteristics of the underlying motionless layer:

$$\begin{aligned} \bar{u} &= 0 \\ \bar{v} &= 0 \\ \bar{T} &= -\Gamma h \end{aligned} \tag{32}$$

where $\Gamma = d\bar{T}/dz$ is the constant temperature gradient in the stably stratified fluid below the mixed layer (see Fig. 1). By definition, the bottom of the thermocline at $z = -h(t)$ is the level beyond which thermals do no penetrate. The thermals' vertical velocity therefore vanishes at that level:

$$w' = 0. \tag{33}$$

Strictly, w' ought to be equal to $-dh/dt$, the rate of entrainment at which the bottom of the thermocline deepens. However, the thermals' sinking velocity through the water column is much greater than the rate of deepening of the thermocline, and boundary condition (33) is a valid approximation.

As pointed out by Thompson (private communication), boundary condition (33) excludes the presence of internal gravity waves, which are generated by tubulent motions in the mixed layer (Linden, 1975; Manins, 1977). The dissipative action of these waves falls outside the scope of the present work and is not included in the model. It is worth noting that a no-flux boundary condition ($\overline{pw} = p_{\rm rms}\, w_{\rm rms} = 0$ at the bottom of the thermocline) is equivalent to (33).

The set of equations requires seven boundary conditions, whereas eight are presently prescribed. The extra condition is precisely the one which will yield a prognostic equation for the mixed-layer depth $h(t)$. The system is thus closed and self-consistent.

5. The hypothesis of a turbulent erosion model (TEM)

For the present boundary conditions, the turbulent kinetic energy input at the surface by the wind is:

$$F_s = -\frac{1}{2}\,\overline{(w-\overline{w})[(u-\overline{u})^2+(v-\overline{v})^2+(w-\overline{w})^2]} - \frac{1}{\rho_0}\,\overline{(w-\overline{w})(p-\overline{p})}$$
$$= -mw_{\mathrm{rms}}(u_{\mathrm{rms}}^2+v_{\mathrm{rms}}^2+w_{\mathrm{rms}}^2) - \frac{1}{\rho_0}\,w_{\mathrm{rms}}\,p_{\mathrm{rms}}$$
$$= mu_*^3 \qquad (34)$$

at $z=0$. Thus the coefficient m as defined by (24) is equivalent to the parameter m_0 as defined by Niiler (1975).

In the case of no dissipation, the turbulent kinetic energy budget (2) is given by Niiler (1975), de Szoeke and Rhines (1976), Niiler (1977):

$$\tfrac{1}{4}N^2h^2\dot{h} = mu_*^3 + \tfrac{1}{2}(\overline{\overline{u}}^2+\overline{\overline{v}}^2)\,\dot{h} \qquad (35)$$

where $\dot{h}=dh/dt$ is the rate of deepening, and the double bar represents a vertical average of mean quantities across the mixed layer. A turbulent erosion model (TEM) balances, in (35), the left-hand side with the first term on the right-hand side, arguing that deepening is caused by erosive action of turbulence propagating from the surface down to the thermocline. A dynamic instability model (DIM), on the other hand, balances, in (35), the left-hand side with the second term on the right-hand side, arguing that deepening results from a shear instability across the thermocline. The computations of de Szoeke and Rhines (1976) show that the DIM holds for times of the order of the inertial period $2\pi/f_0$. At later times, the mass flow in the mixed layer is limited to the Ekman transport, the velocity components $\overline{\overline{u}}$ and $\overline{\overline{v}}$ decrease as h^{-1}, and a TEM applies.

Because this study is directed toward long time scales, assumptions will be made to reduce the model to a TEM, and thus decouple the mixed-layer deepening from the mean horizontal flow. As a result, a simple analytical solution will be found. The pressure term in eq. (22) represents the mechanism of production of turbulent kinetic energy from the mean flow shear (Cushman-Roisin, 1981). The reduction of the model to a TEM is thus accomplished mathematically by neglecting the pressure term in (22). The final model thus reduces to the following set of equations:

$$\frac{\partial \overline{T}}{\partial t} = -\frac{\partial}{\partial z}(w_{\mathrm{rms}}T_{\mathrm{rms}}) \qquad (36)$$

$$\frac{\partial}{\partial z}(\overline{T}+mT_{\mathrm{rms}}) = 0 \qquad (37)$$

$$\frac{\partial \overline{u}}{\partial t} - f_0\overline{v} = -\frac{\partial}{\partial z}(u_{\mathrm{rms}}w_{\mathrm{rms}}) \qquad (38)$$

$$\frac{\partial \overline{v}}{\partial t} + f_0\overline{u} = -\frac{\partial}{\partial z}(v_{\mathrm{rms}}w_{\mathrm{rms}}) \qquad (39)$$

$$\frac{\partial}{\partial z}(\overline{u}+2mu_{\mathrm{rms}}) = 0 \qquad (40)$$

$$\frac{\partial}{\partial z}(\overline{v}+2mv_{\mathrm{rms}}) = 0 \qquad (41)$$

$$3mw_{\mathrm{rms}}\frac{\partial w_{\mathrm{rms}}}{\partial z} = \alpha g T_{\mathrm{rms}} \qquad (42)$$

with the boundary conditions at $z=0$:

$$T_{\mathrm{rms}} = 0 \qquad (43)$$

$$u_{\mathrm{rms}} = \tau_x/(\rho_0 u_*) \qquad (44)$$

$$v_{\mathrm{rms}} = \tau_y/(\rho_0 u_*) \qquad (45)$$

$$w_{\mathrm{rms}} = -u_* \qquad (46)$$

and at $z=-h$:

$$\overline{T} = -\Gamma h \qquad (47)$$

$$\overline{u} = 0 \qquad (48)$$

$$\overline{v} = 0 \qquad (49)$$

$$w_{\mathrm{rms}} = 0. \qquad (50)$$

6. Change of variable and functions

Since the mixed layer is constantly deepening, it is advantageous to use the similarity variable $\xi=-z/h(t)$ which varies from zero at the surface to one at the bottom of the thermocline.

On the other hand, one may immediately

integrate equations (37), (40) and (41) with respect to z and define:

$$\bar{u} = U(t) - 2m\tilde{u}(t, \xi) \qquad u_{\text{rms}} = \tilde{u}(t, \xi) \tag{51}$$

$$\bar{v} = V(t) - 2m\tilde{v}(t, \xi) \qquad v_{\text{rms}} = \tilde{v}(t, \xi) \tag{52}$$

$$\bar{T} = -\Gamma T(t) - m\Gamma\tilde{T}(t, \xi) \quad T_{\text{rms}} = \Gamma\tilde{T}(t, \xi) \tag{53}$$

where tilded quantities are ξ and t-dependent and represent rms quantities. The non-tilded quantities U, V and T are constants of integration and depend upon time only. They will have to be determined by the boundary conditions. Note that due to the presence of the factor Γ, the new temperature variables $T(t)$ and $\tilde{T}(t,\xi)$ have the dimension of a length. The rms vertical velocity may be redefined as:

$$w_{\text{rms}} = -\tilde{w}(t, \xi) \tag{54}$$

in order to work with a positive variable.

With these changes of variable and functions, the remaining governing equations (36), (38), (39) and (42) become:

$$-\dot{T} - m\frac{\partial\tilde{T}}{\partial t} + m\frac{\dot{h}}{h}\xi\frac{\partial\tilde{T}}{\partial\xi} = -\frac{1}{h}\frac{\partial}{\partial\xi}(\tilde{w}\tilde{T}) \tag{55}$$

$$\dot{U} - 2m\frac{\partial\tilde{u}}{\partial t} + 2m\frac{\dot{h}}{h}\xi\frac{\partial\tilde{u}}{\partial\xi} - f_0 V + 2mf_0\tilde{v} = -\frac{1}{h}\frac{\partial}{\partial\xi}(\tilde{u}\tilde{w}) \tag{56}$$

$$\dot{V} - 2m\frac{\partial\tilde{v}}{\partial t} + 2m\frac{\dot{h}}{h}\xi\frac{\partial\tilde{v}}{\partial\xi} + f_0 U - 2mf_0\tilde{u} = -\frac{1}{h}\frac{\partial}{\partial\xi}(\tilde{v}\tilde{w}) \tag{57}$$

$$3m\tilde{w}\frac{\partial\tilde{w}}{\partial\xi} = -N^2 h\tilde{T} \tag{58}$$

where $N^2 = \alpha g\Gamma$ is the square of the Brunt–Väisälä frequency in the underlying stratum, and where a dot represents a time derivative. The boundary conditions become:

$$\tilde{T}(0) = 0, \quad \tilde{u}(0) = \tau_x/(\rho_0 u_*), \quad \tilde{v}(0) = \tau_y/(\rho_0 u_*), \quad \tilde{w}(0) = u_* \tag{59}$$

and

$$\tilde{T}(1) = (h - T)/m, \quad \tilde{u}(1) = U/2m, \quad \tilde{v}(1) = V/2m, \quad \tilde{w}(1) = 0. \tag{60}$$

This constitutes a set of four coupled first-order non-linear differential equations which require four boundary conditions. However, they contain four unknown time-dependent functions: $T(t)$, $U(t)$, $V(t)$ and $h(t)$, for which four additional conditions are required. The system consists of eight boundary conditions, precisely what is required.

7. Richardson numbers

The global heat budget of the mixed layer and thermocline, integrated over time, expresses that the temperature difference from the initial value integrated over the water column is equal to the time integration of the net surface heat flux. It thus follows from (53), (55) and (58) that $T(t)$ is given by:

$$T(t) = \frac{h}{2}\left(1 - 3m^2\frac{u_*^2}{N^2 h^2}\right). \tag{61}$$

For oceanic values corresponding to time scales greater than the inertial period, i.e.,

$N \sim 10^{-2}\,\text{s}^{-1}$, $u_* \sim 10^{-2}\,\text{ms}^{-1}$,
$h \gtrsim 20$ m, m of the order one,

it is easily seen that the second term in the parentheses in (61) is of order of 10^{-2}. Therefore, because the mixed layer is deep enough ($h \gg u_*/N$), the heat budget reduces at the leading order to:

$$T = \frac{h}{2}. \tag{62}$$

If $\Delta\rho$ is the density jump across the thermocline, and ρ_0 the reference density, the total buoyancy in the mixed layer is:

$$B = g\frac{\Delta\rho}{\rho_0}h = \frac{N^2 h^2}{2} \tag{63}$$

by virtue of (62).

The mixed-layer deepening under the action of a surface wind stress is successfully characterized by the values of two Richardson numbers, ratios of the total buoyancy in the mixed layer to the square of a velocity. The *frictional Richardson number* is the ratio of B as defined by (63) to the square of the friction velocity u_* as defined by (29), based on the wind-stress amplitude:

$$Ri = \frac{N^2 h^2}{2u_*^2}. \tag{64}$$

This is the Richardson number used by Turner and Kraus (1967), Kato and Phillips (1969), Kim (1976), Kullenberg (1977) and Price, Mooers and Van Leer (1978). The *shear Richardson number* is the ratio of B to the square of the mean horizontal velocity difference across the thermocline, here approximated by $U^2 + V^2$, as introduced by (51) and (52):

$$R_v = \frac{N^2 h^2}{2(U^2 + V^2)}.$$

R_v is the Richardson number used by Pollard, Rhines and Thompson (1973), Garwood (1977), Dillon and Powell (1979), Price (1979) and Kundu (1980).

Both numbers Ri and R_v are time-dependent through h, U and V and increase as the mixed layer deepens. They characterize at any time the state of the system. The frictional number, Ri, is the dominant number in TEM's, for turbulence induced by vertical shear across the thermocline is neglected compared to the surface input. Because the present model is a TEM, the frictional Richardson number, Ri, will play an essential role. It increases from zero, when the wind starts to blow, to values much larger than unity, when the mixed layer is well-developed ($Ri \sim 10^2$ for orders of magnitude listed above in this section). The shear Richardson number is also time-varying but is of the order of one.

Mathematically, it will be assumed here that the mixed-layer + thermocline system may be treated as an interior + boundary-layer problem. It will be shown *a posteriori* that this simplification holds when

$$Ri \gg 1$$

i.e., when the mixed layer is well developed.

Another important dimensionless number is the rate of entrainment

$$E = \frac{\dot{h}}{u_*} \tag{66}$$

the ratio of the deepening rate to the friction velocity, as defined by Kato and Phillips (1969). The friction velocity is characteristic of the vertical downward velocity of thermals. It is anticipated to be large compared to the rate of deepening of the thermocline because thermals take a short time to sink from the surface down to the thermocline compared to the time scale of evolution of the whole system. The entrainment parameter is thus expected to be very small compared to one.

Finally, a last dimensionless time-dependent number can be defined by:

$$\varepsilon = \frac{u_*}{(U^2 + V^2)^{1/2}} = \left(\frac{R_v}{Ri}\right)^{1/2} \tag{67}$$

This number can be interpreted as a drag coefficient (Kitaigorodskii, 1981) and is small compared to one.

Dimensional analysis (Kitaigorodskii, 1981) implies that the solution of the mixed-layer deepening can be written in the form:

$$E = F(Ri, \varepsilon)$$

where F is a universal function. In the present model, turbulence production by shear in the thermocline is neglected, and, as a result, the vertical-momentum equation is decoupled from the horizontal-momentum equations. The rate of deepening, E, is thus found to be independent of the horizontal velocity, and the function F will not depend upon ε.

8. Solution

8.1. *Hypotheses of a quasi-homogeneous mixed layer*

It is well known from observations and laboratory experiments that when the mixed layer is well developed, it is quasi-homogeneous and bounded below by a thin layer of large gradients, called the thermocline. This behavior may be anticipated *a priori* and a boundary-layer treatment is therefore the appropriate method of solution. The system is divided into two regions, the interior region where the horizontal velocity and temperature are almost constant with depth

$$\tilde{u} \ll U, \quad \tilde{v} \ll V, \quad \tilde{T} \ll T, \qquad \frac{\partial}{\partial \xi} = 0(1) \tag{68}$$

and the thermocline, where vertical gradients are anticipated to be very large:

$$\tilde{u} \sim U, \quad \tilde{v} \sim V, \quad \tilde{T} \sim T, \qquad \frac{\partial}{\partial \xi} \gg 0(1). \tag{69}$$

These assumptions will be verified *a posteriori*, and it will be shown that they are correct provided that Ri is much greater than one.

8.2. *Solution in the mixed layer*

Assuming a quasi-homogeneous mixed layer, eqs. (55) to (58) reduce to:

$$-\dot{T} = -\frac{1}{h}\frac{\partial}{\partial \xi}(\tilde{w}\tilde{T}) \tag{70}$$

$$\dot{U} - f_0 V = -\frac{1}{h}\frac{\partial}{\partial \xi}(\tilde{u}\tilde{w}) \tag{71}$$

$$\dot{V} + f_0 U = -\frac{1}{h}\frac{\partial}{\partial \xi}(\tilde{v}\tilde{w}) \tag{72}$$

$$3m\tilde{w}\frac{\partial \tilde{w}}{\partial \xi} = -N^2 h\tilde{T}. \tag{73}$$

The left-hand sides of the first three equations are independent of ξ. Integrations with respect to ξ and use of surface boundary conditions (59) yield:

$$\tilde{T} = \frac{h\dot{T}\xi}{\tilde{w}} \tag{74}$$

$$\tilde{u} = \frac{\tau_x/\rho_0 - h(\dot{U} - f_0 V)\,\xi}{\tilde{w}} \tag{75}$$

$$\tilde{v} = \frac{\tau_y/\rho_0 - h(\dot{V} + f_0 U)\,\xi}{\tilde{w}}\,. \tag{76}$$

Replacing $\tilde{T}$ by (74) in eq. (73) yields a single equation for $\tilde{w}$ whose solution is:

$$\tilde{w}^3 = u_*^3 - \frac{N^2 h^2 \dot{T}}{2m}\,\xi^2 \tag{77}$$

after the surface boundary condition (59) has been used.

8.3. *Solution in the thermocline*

The dominant terms in the governing equations are now those which include derivatives with respect to ξ. Moreover, since this boundary layer lies near $\xi = 1$, ξ may be replaced by one where it appears. Equations (55) to (58) now reduce to:

$$m\frac{\dot{h}}{h}\frac{\partial \tilde{T}}{\partial \xi} = -\frac{1}{h}\frac{\partial}{\partial \xi}(\tilde{w}\tilde{T}) \tag{78}$$

$$2m\frac{\dot{h}}{h}\frac{\partial \tilde{u}}{\partial \xi} = -\frac{1}{h}\frac{\partial}{\partial \xi}(\tilde{u}\tilde{w}) \tag{79}$$

$$2m\frac{\dot{h}}{h}\frac{\partial \tilde{v}}{\partial \xi} = -\frac{1}{h}\frac{\partial}{\partial \xi}(\tilde{v}\tilde{w}) \tag{80}$$

$$3m\tilde{w}\frac{\partial \tilde{w}}{\partial \xi} = -N^2 h\tilde{T}. \tag{81}$$

These last equations may be easily integrated with respect to ξ. The constants of integration are determined by using the bottom boundary conditions (60):

$$\tilde{T} = \frac{(h-T)\,\dot{h}}{\tilde{w} + m\dot{h}} \tag{82}$$

$$\tilde{u} = \frac{\dot{h}U}{\tilde{w} + 2m\dot{h}} \tag{83}$$

$$\tilde{v} = \frac{\dot{h}V}{\tilde{w} + 2m\dot{h}} \tag{84}$$

where $\tilde{w}$ is implicitly given by the cubic polynomial:

$$\tilde{w}^3 + \tfrac{3}{2}m\dot{h}\tilde{w}^2 = \frac{N^2 h(h-T)\,\dot{h}}{m}\,(1-\xi). \tag{85}$$

8.4. *Matching of solutions*

The two sets of solutions were obtained independently for the mixed layer and thermocline by using surface and bottom boundary conditions, respectively. However, they ought to be the asymptotic forms of a unique set of solutions valid throughout the whole water column. This requires imposing matching conditions. As a result, four prognostic equations for the time-dependent functions T, U, V and h will be obtained.

Mathematically, matching conditions are obtained by writing that, for each variable $\tilde{T}$, $\tilde{u}$, $\tilde{v}$ and $\tilde{w}$, the mixed layer solution for ξ approaching unity is equal to the thermocline solution for $\tilde{w}$ much greater than $\dot{h}$. The resulting relations are:

$$\frac{h\dot{T}}{\tilde{w}} = \frac{(h-T)\,\dot{h}}{\tilde{w}}$$

$$\frac{\tau_x/\rho_0 - h(\dot{U} - f_0 V)}{\tilde{w}} = \frac{\dot{h}U}{\tilde{w}}$$

$$\frac{\tau_y/\rho_0 - h(\dot{V} + f_0 U)}{\tilde{w}} = \frac{\dot{h}V}{\tilde{w}}$$

$$u_*^3 - \frac{N^2 h^2 \dot{T}}{2m} + \frac{N^2 h^2 \dot{T}}{m}(1-\xi) = \frac{N^2 h(h-T)\,\dot{h}}{m}(1-\xi)\,\cdot$$

The above equations can be rewritten as:

$$(hT)^{\bullet} = h\dot{h} \tag{86}$$

$$(hU)^{\bullet} - f_0(hV) = \frac{\tau_x}{\rho_0} \tag{87}$$

$$(hV)^{\bullet} + f_0(hU) = \frac{\tau_y}{\rho_0} \tag{88}$$

$$N^2 h^2 \dot{T} = 2mu_*^3. \tag{89}$$

Equation (86) can be integrated over time in order to obtain T in terms of h:

$$T = \frac{h}{2}\left(1 + \frac{\text{constant}}{h^2}\right). \tag{90}$$

The constant of integration cannot be determined by the initial conditions, since the boundary-layer technique breaks down at the incipient deepening, when the mixed layer and thermocline are not well defined. But, eq. (90) is identical to the global heat budget (61), which is an exact result for all times. The constant of integration is therefore $-3m^2u_*^4/N^2$ and,

$$T = \frac{h}{2}\left(1 - \frac{3m^2}{2Ri}\right) \tag{91}$$

which reduces to (62), because Ri is much greater than one.

Equations (87) and (88) are the classical transport equations, whose general solution contains inertial oscillations superimposed on an Ekman drift to the right of the wind stress. For a time-dependent wind stress, the solution is:

$$hU = h_0 U_0 + \frac{1}{\rho_0}\int_0^t [\tau_x(\tau)\cos f_0(t-\tau) + \tau_y(\tau)\sin f_0(t-\tau)]\, d\tau$$

$$hV = h_0 V_0 + \frac{1}{\rho_0}\int_0^t [\tau_y(\tau)\cos f_0(t-\tau) - \tau_x(\tau)\sin f_0(t-\tau)]\, d\tau.$$

The last relation (89) combined with (91) is the prognostic equation for the mixed-layer depth, and is discussed in the next section. Finally, the vertical profiles valid throughout the water column are:

$$\tilde{T} = \frac{h\dot{T}\xi}{m\dot{h} + \tilde{w}} \tag{92}$$

$$\tilde{u} = \frac{\tau_x/\rho_0(1-\xi) + \dot{h}U\xi}{\tilde{w} + 2m\dot{h}} \tag{93}$$

$$\tilde{v} = \frac{\tau_y/\rho_0(1-\xi) + \dot{h}V\xi}{\tilde{w} + 2m\dot{h}} \tag{94}$$

where $\tilde{w}$ is implicitly given by:

$$\tilde{w}^3 + \tfrac{3}{2}m\dot{h}\tilde{w}^2 = u_*^3(1-\xi^2). \tag{95}$$

It is evident from the structure of this final solution, (92) to (95), that the solution is not similar. None of the variables can be expressed as single products of time dependent and ξ-dependent functions. Kundu (1981) has shown that a similarity solution can exist. However, the model is highly non-linear, and the solution is not unique. It can be shown (personal work, in preparation) that, in the case of an initially linear stratification which is treated here, the similarity solution is unstable and tends to deform itself into a steplike solution, i.e., the solution which has been found here.

9. Mixed-layer deepening

Equations (91) and (89) form a coupled set of equations for T and h. Eliminating T, a prognostic equation for h is obtained:

$$(N^2h^2 + 3m^2u_*^4)\dot{h} = 4mu_*^3 \tag{96}$$

which reduces to

$$N^2h^2\dot{h} = 4mu_*^3 \tag{97}$$

since it was assumed that $Ri \gg 1$. This last equation is the turbulent kinetic energy budget for a TEM without dissipation, expressing that the time rate of change of potential energy equals the turbulent kinetic energy input by wind at the surface. If the wind-stress amplitude is constant with time, the mixed-layer depth increases in time as $t^{1/3}$.

In a dimensionless form, (96) and (97) become:

$$E = \frac{2m}{3m^2/2 + Ri} \tag{98}$$

and

$$E = \frac{2m}{Ri} \tag{99}$$

respectively, where E and Ri are defined by (66) and (64). The dependence of the entrainment rate on the inverse of the frictional Richardson number has long been observed in the laboratory (Kato and Phillips, 1969) as well as in oceans and lakes (Kullenberg, 1977; Price et al., 1978; Dillon and Powell, 1979).

Various values of m are proposed by authors, and more can be computed from data in the literature. A summary of values computed for the case of deepening in a stratified fluid is shown in Table 1. From the table, one concludes that all the values of m agree rather well: approximately one or slightly larger. Scattering can be attributed to dissipation or to the influence of the initial conditions. Values of f, the fraction of area occupied by thermals, were computed by (24) and are of the order of 10%. Thermals are thus rather small disturbances within a return flow which occupies most of the available surface. This result agrees with numerical calculations (Piacsek, 1968) and laboratory observations (Turner, 1973), which all show that thermals or plumes are narrow and occupy a small fraction of the total area at any level. For a system where the roles played by thermals and anti-thermals are perfectly symmetric, one can argue that the value of f ought to be 50%. However, in the present situation, thermals are locally generated very near the surface while anti-thermals are progressively formed in the water column as they rise, and an excess of momentum is input locally at the surface, while it is progresively consumed for an evenly-distributed momentum increase of the water column. These asymmetries explain why thermals are narrow and anti-thermals diffuse and thus why f differs markedly from 50%.

The correction in the denominator of (98) is reminiscent of the one proposed by Kim (1976):

$$E = \frac{2m}{(c_m/u_*)^2 + Ri}$$

where $\frac{1}{2}c_m^2$ is the average turbulent kinetic energy across the mixed layer. For $m = 1.25$, Kim proposes $(c_m/u_*)^2 = 9$, while (98) yields $3m^2/2 = 2.34$. The corrections are thus of the same order of magnitude.

The results of this section permit justification of the assumptions which were stated before solving the equations. One has to show that the approximations

$$\tilde{T} \ll T, \quad \tilde{u} \ll U, \quad \tilde{v} \ll V$$

hold in the mixed layer as long as $Ri \ll 1$. In the mixed layer, $\tilde{w}$ is of order of u_*, its surface value, which is much larger than $\dot{h}$ according to (99). From (92), (93) and (94), one obtains:

$$\frac{\tilde{T}}{T} \sim \frac{\tilde{u}}{U} \sim \frac{\tilde{v}}{V} \sim \frac{\dot{h}}{u_*} \sim Ri^{-1} \ll 1$$

which validates the method of solution chosen for this problem.

10. Thickness of the thermocline

Due to non-linearities, the boundary-layer method applied here differs from classical applications to linear systems, and caution must be exercised when one evaluates the boundary-layer thickness. At first, one could think that the thermocline is the region were $\tilde{w}$ is of order $\dot{h}$, so that corrections in the denominators of (92) to

Table 1. *Values of the coefficient m found in the literature or computed from published data. The values of the frictional Richardson number for which the data were taken and the values of f computed from (24) are also given*

Year	Author(s)	Data	Ri	m	f
1969	Kato and Phillips	Laboratory experiments	15–400	1.25	0.11
1969	Turner	South of Bermuda	30	1.64	0.07
1973	Denman and Miyake	Station Papa	150	1.0	0.15
1974	Halpern	Northeast Pacific	80	2.8	0.03
1977	Kullenberg	Coastal waters—Lakes	10–10^4	1.1	0.13
1978	Price et al.	West Florida cont. shelf	300	0.9	0.17
1979	Dillon and Powell	Lake Tahoe, CA-NV	30	0.90–1.6	0.03–0.17

(94) become important. This argument leads to a dimensionless thermocline thickness of order Ri^{-3}, which is much too small. There is a thicker layer where boundary corrections start to appear in the solution. Indeed, in the temperature equation (55),

$$-\dot{T} - m\frac{\partial \tilde{T}}{\partial t} + m\frac{\dot{h}}{h}\xi\frac{\partial \tilde{T}}{\partial \xi} = -\frac{1}{h}\frac{\partial}{\partial \xi}(\tilde{w}\tilde{T})$$

(a) (b) (c) (d)

the right-hand side, term (d), balances term (a) in the mixed layer, while it balances term (c) in the thermocline. The top of the thermocline is thus the level where term (c) begins to take over term (a). Boundary corrections therefore start to appear where these two terms compete, i.e., where

$$\dot{T} \sim \frac{\dot{h}}{h}\xi\frac{\tilde{T}}{\delta\xi}$$

where $\delta\xi$ is the dimensionless thermocline thickness. Because the boundary layer is a thin region, ξ is almost one, and, according to (89) and (92), $\tilde{T}$ is of order of $(hu_*)/(Ri\tilde{w})$, so that:

$$\delta\xi \sim \frac{u_*}{Ri\tilde{w}}. \tag{100}$$

The balance of the vertical-momentum equation (58) combined with (89) requires:

$$\frac{\tilde{w}^2}{\delta\xi} \sim \frac{u_*^3}{\tilde{w}}. \tag{101}$$

Finally, combination of (100) with (101) yields:

$$\delta\xi \sim Ri^{-3/4}, \tag{102}$$

$$\tilde{w} \sim u_* Ri^{-1/4}. \tag{103}$$

Therefore the dimensionless thickness of the thermocline is $Ri^{-3/4}$ rather than Ri^{-3}.

In a study of turbulence and entrainment within the interfacial zone bounding a mixed layer, Long (1978) proposes a series of arguments to relate turbulent velocities, temperature fluctuations, thermocline thickness, and other variables to the frictional Richardson number. Although his results are drawn in the case of turbulence generation at the surface by an oscillating grid, it is possible (see Appendix B) to apply his arguments to the present case. From this analysis, it is concluded that Long's arguments, too, lead to a thermocline thickness and a rms vertical velocity of the order of $hRi^{-3/4}$, and $u_* Ri^{-1/4}$, respectively. The agreement between the two approaches is perfect and supports the modelling by two interacting fluids as a theory of convective turbulence.

The actual dimensional thickness of the thermocline is:

$$h\delta\xi = \left(\frac{u_*}{N}\right)^{3/2} h^{-1/2} \tag{104}$$

and decreases as the mixed layer deepens. This interface shallowing was observed in laboratory experiments (Kato and Phillips, 1969) and in numerical experiments (Kundu, 1980).

11. Vertical profiles

Solutions (92) to (95) govern the vertical variations of rms fluctuations throughout the mixed layer and thermocline. They can be used in (51) to (54) to yield the profiles of mean quantities; they can also be combined to form vertical fluxes.

Figs. 3 to 10 are plots of vertical profiles of physical quantities of interest. The wind stress is taken in the x-direction:

$$\tau_x/\rho_0 = u_*^2$$

$$\tau_y/\rho_0 = 0$$

and mean currents at 45° to its right:

$$U = -V = ku_*.$$

The values assigned to the various parameters are:

$Ri = 100$, $m = 1.25\ (f = 0.11)$, $k = 7$

Fig. 3 is a plot of the turbulent vertical velocity, which is proportional to the thermals' vertical velocity. Thermals leave the surface with the friction velocity imposed by the surface stress. As they sink, they become slightly buoyant and decelerate. Their velocity vanishes precisely at the bottom of the thermocline.

Fig. 4 shows the mean temperature profile. The temperature is almost homogeneous in the mixed layer and equal to $-\Gamma h/2$, as required by heat conservation. There is however a slight stable gradient of order Ri^{-1}, so that thermals progresively become buoyant and decelerate as they sink through the mixed layer. The thermocline is well defined, and its thickness corresponds to (102). Fig. 5 shows the development of the mixed

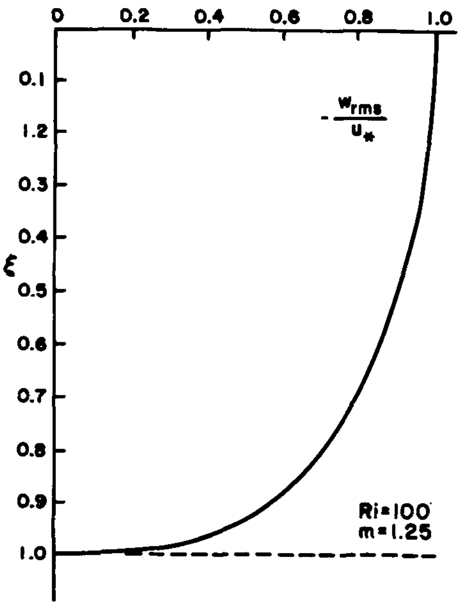

Fig. 3. Profile of turbulent vertical velocity, scaled by the friction velocity.

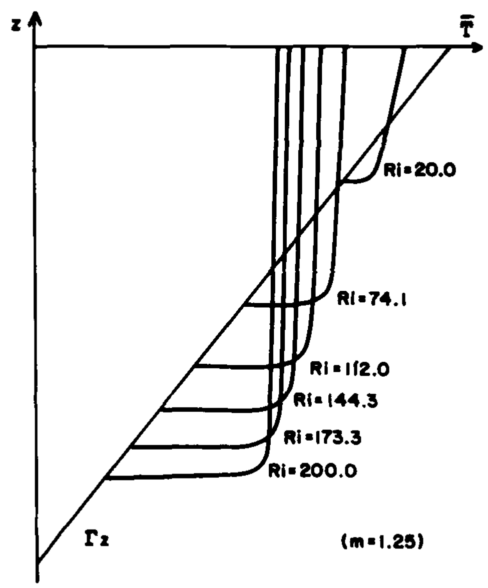

Fig. 5. Development of the mixed layer. Constant time intervals separate mean temperature profiles.

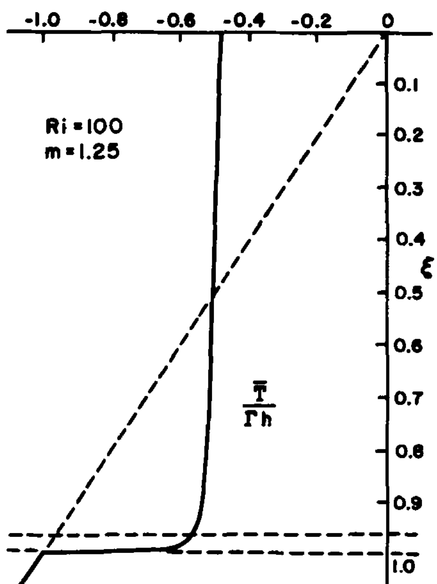

Fig. 4. Mean temperature profile.

layer and the shallowing of the thermocline as time goes on.

Figs. 6a and b show the vertical profiles of the horizontal velocity components, $\bar{u}$ and $\bar{v}$. The mixed layer is quasi-homogeneous as required by the assumptions made in order to solve the governing equations analytically. This excludes Ekman veering with depth, and separates the flow into a depth-independent inertial oscillation and a quasi-steady shearing flow that carries the turbulent stresses downward through the mixed layer. This is similar to the results of Kundu (1980) for time scales greater than the inertial period, when his model becomes a TEM. The velocity $\bar{u}$ in the direction of the surface stress increases slightly with depth. The reason is the following: as thermals sink, they progressively exchange with anti-thermals the extra momentum they have received near the surface. This reduces the turbulent fluctuations, and increases the mean value accordingly. The $\bar{v}$-profile does not exhibit such behavior since there is no extra-momentum in the y-direction given at the surface. In the thermocline, both profiles curve sharply and vanish so as to match the bottom boundary conditions.

Figs. 7a and b show the vertical profiles of the Reynolds stresses, $-\overline{uw}$ and $-\overline{vw}$, scaled by the surface stress. Both stresses vary linearly through the mixed layer, from the imposed value at the surface, to a residual value at the top of the thermocline. These residual values are $\dot{h}U$ and $\dot{h}V$, and are precisely the jump conditions imposed by

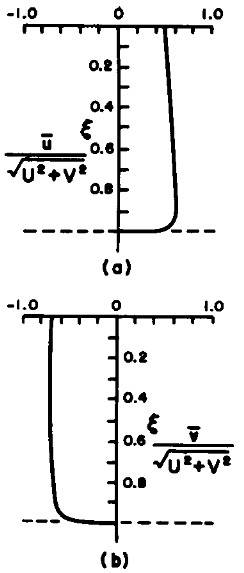

Figs. 6a and b. Profiles of mean horizontal velocity components, scaled by $\sqrt{U^2 + V^2}$; $\bar{u}$ is in the direction of the imposed wind-stress.

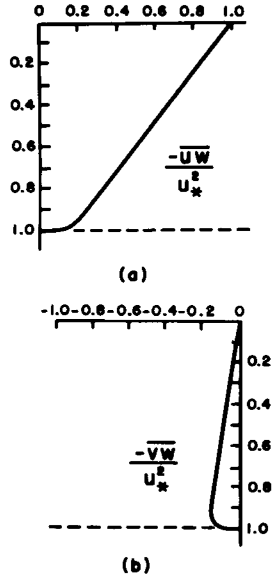

Figs. 7a and b. Profiles of the Reynolds stresses $-\overline{uw}$ and $-\overline{vw}$, scaled by the surface stress u_*^2 in the x-direction.

authors of bulk models (Niiler, 1975, for example). The stresses decrease rapidly through the thermocline to zero so as to meet bottom boundary conditions.

From mean profiles and stresses, one can compute eddy viscosities defined by:

$$\nu_u = \frac{-\overline{uw}}{\partial \bar{u}/\partial z} \quad \text{and} \quad \nu_v = \frac{-\overline{vw}}{\partial \bar{v}/\partial z}.$$

Figs. 8a and b show the results. The eddy viscosity in the x-direction is negative in the mixed layer due to the increase of $\bar{u}$ with depth. The negative values are correlated with a transfer of momentum from turbulent motions to mean current. The turbulence generated at the surface by the wind is progressively structured to increase the mean current. In the y-direction, no turbulence is supplied at the surface, and fluctuations increase downward due to differences between sinking thermals and rising anti-thermals. At the level where $\bar{u}$ is maximum, a little above the thermocline, ν_u is unbounded, as a result of its definition. Below that level, in the thermocline, the strong shear of the mean flow generates turbulence, and eddy viscosities are both positive. They vanish at the bottom of the thermocline, where stresses vanish, and shear is maximum. It is worth noting that ν_u is quasi-constant near the surface, and that ν_v increases linearly from the surface like

$$\nu_v \sim \frac{u_*}{2m} |z|$$

in agreement with the clasical theory of turbulence. The corresponding Von Kármán constant is

$$\kappa = \frac{1}{2m} = 0.40$$

for $m = 1.25$. This result is encouraging. There is therefore a link between the parameter m and the Von Kármán constant. The laboratory value obtained for m is in perfect agreement with laboratory measurements of turbulent flow.

Fig. 9 shows the profile of the vertical convective heat flux. Mixing brings cold water from below, cools the surface layers and heats the fluid recently entrained in the convective process. There is therefore downward transfer of heat. This is the reason why the heat flux is negative everywhere. The constant gradient through the mixed layer corresponds to a homogeneous cooling of the fluid, as stated by the heat eq. (15). The maximum negative value at the top of the thermocline

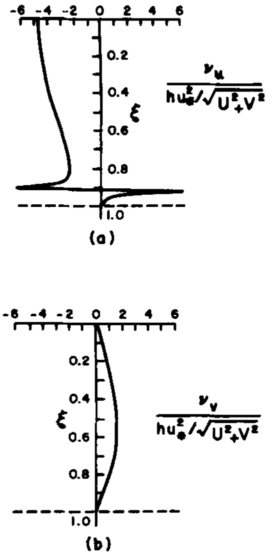

Figs. 8a and b. Profiles of the eddy viscosities ν_u and ν_v (cf. text), scaled by $hu_*^2/\sqrt{U^2+V^2}$.

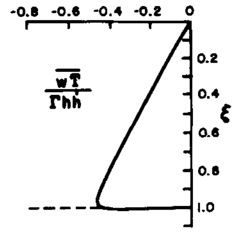

Fig. 9. Profile of the vertical convective heat flux $\overline{wT}$, scaled by $\Gamma h\dot{h}$.

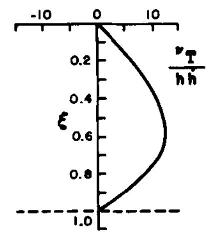

Fig. 10. Profile of the eddy heat diffusivity ν_T (cf. text), scaled by $h\dot{h}$.

is close to $-\frac{1}{2}\Gamma h\dot{h}$, which is the jump condition across the thermocline, used in bulk models (Kraus and Turner, 1967, for example).

Fig. 10 shows the profile of the eddy heat diffusivity defined by

$$\nu_T = \frac{-\overline{wT}}{\partial\overline{T}/\partial z}$$

It is positive everywhere, and has a profile similar to the one of ν_v.

12. Monin–Obukhov length

The Monin–Obukhov length can be interpreted as a local and instantaneous length scale, over which turbulence generated by release of potential energy is comparable to the mechanically-induced turbulence. It is generally defined as (Turner, 1973; Zilitinkevich et al., 1979):

$$l = \frac{u_*^3}{\kappa\mathfrak{B}}$$

where u_* is the friction velocity characteristic of the turbulence, κ the Von Kármán constant, and $\mathfrak{B}$ the vertical buoyancy flux.

In the present case, the vertical buoyancy flux is noted

$$\mathfrak{B} = \alpha g\,|\,\overline{wT}\,|$$

which is zero at the surface and at the bottom of the thermocline. It is maximum near the top of the thermocline. The value of that maximum is obtained (at the leading order in Ri^{-1}) as the limit of the mixed-layer buoyancy flux as ξ tends to one:

$$\mathfrak{B} = \lim_{\xi\to 1} \alpha g\,|\,\overline{wT}\,| = N^2 h\dot{T}$$

by using (10), (14) and (74). Using this maximum value in the definition of l, one obtains the smallest Monin–Obukhov length which can be defined:

$$l = \frac{u_*^3}{\kappa N^2 h\dot{T}} = \frac{1}{2\kappa m}\,h$$

by virtue of (89). The Monin–Obukhov length is therefore proportional to h. The coefficient of proportionality $(2\kappa m)^{-1}$ equals unity for $\kappa = 0.40$ and $m = 1.25$. This result has a physical reason: the wind-mixed layer is a convective system generated by surface turbulence; therefore, turbulence and convection have equal importance, and the Monin–Obukhov length has to be proportional to and of order of the depth of the layer, i.e., h.

Inversely, this physical argument could have been used independently, by writing *a priori* $l = h$ (Zilitinkevich et al., 1979). The model would therefore conclude that $(2\kappa m)^{-1}$ equals one, or

$$m = 1.25$$

for $\kappa = 0.40$. The value of m can therefore be inferred from the theory, and be compared to observations and laboratory experiments (see Table 1). The agreement is excellent.

When a buoyancy flux (cooling or heating) is imposed at the surface, convection or restratification may dominate turbulence. In such a case, the Monin–Obukhov length is expected to be small or larger than h (Kantha, 1980), and the resulting values of m are expected to be greater or smaller than 1.25.

13. Conclusions

A new model of convection and mixing is applied to the study of mixed-layer deepening under the action of wind stress. It is based on a modelling by two interacting fluids. Emphasis is not on the energetics, but rather on the dynamics of mixing. Turbulence production by mean shear near the thermocline is neglected in order to simplify the vertical-momentum equation. The model is thus a turbulent erosion model, for which the potential-energy increase required for deepening is provided by turbulence input at the surface.

A simple analytical solution is found in the case where the mixed layer is well-mixed and separated from the underlying quiescent fluid by a sharp thermocline. The results are valid if the frictional Richardson number is much greater than unity, the condition for a sharp thermocline to exist. Expressions for the thermocline thickness and turbulence scale near the thermocline are in very good agreement with previous results of turbulence theory.

Vertical profiles are then plotted. The turbulent vertical velocity decreases monotonically from a maximum value at the surface down to zero at the bottom of the thermocline, without showing any sudden variations in the thermocline. The temperature profile is composed of a quasi-constant value through the mixed layer and of a rapid variation in the thermocline. Velocity profiles show the separation of the flow into a depth-independent inertial oscillation and a quasi-steady shearing flow that carries the turbulent stresses downward through the mixed layer. In the thermocline, the profiles curve sharply in order to match the zero mean velocity in the underlying stable fluid. Reynolds stresses and vertical convective heat flux vary linearly through the mixed layer from their respective imposed surface values to residual values required for entraining new fluid in the mixing process. In the thermocline, they rapidly decrease to zero. Resulting eddy diffusivities of heat and momentum are computed and plotted. The eddy viscosity of the flow in the direction of the wind stress is negative near the surface, implying that a part of the turbulent energy supplied at the surface goes to the mean flow. In the direction perpendicular to the surface stress, the eddy viscosity varies like the eddy heat diffusivity, vanishing at the surface and at the bottom of the thermocline, and reaching a maximum somewhere at mid-depth. Finally, an argument based on the proportionality between the Monin–Obukhov length and the mixed-layer depth leads to relating the parameter m, ratio of the turbulent kinetic energy input to the cube of the friction velocity, to the Von Kármán constant. The value is found to be equal to the one proposed by Kato and Phillips (1969) and in good agreement with field observations.

14. Appendix A

The entrainment layer

The results presented in the previous section [eqs. (92) to (95)] were based on the assumption of a constant fraction of area occupied by thermals throughout the mixed layer and thermocline. This, however, leads to some inconsistencies. At the bottom of the thermocline ($z = -h$), the anti-thermals' variables are given by:

$$T'' = -\frac{1-f}{1-2f}\Gamma h$$

$$u'' = -\frac{f}{1-2f}U \qquad \text{(A1)}$$

$$v'' = -\frac{f}{1-2f}V.$$

At that level, however, anti-thermals are constituted of newly entrained fluid, and the expected values are

$$T'' = -\Gamma h, \quad u'' = v'' = 0. \tag{A2}$$

The values (A1) reduce to (A2) if $f = 0$.

Therefore, these inconsistencies can be removed by including a new boundary layer below the thermocline, here named the *entrainment layer*. The role of this layer is to allow f to decrease from its constant value in the mixed layer and thermocline, through this entrainment layer, down to zero in the quiescent fluid underneath it.

The purpose of this appendix is to show that, based on scaling arguments, this entrainment layer is in fact very thin and, thus, cannot have any effect on the dynamics of the whole system.

In a thin layer of large gradients, the mean-temperature equation reduces to (78), implying that the scale for the vertical-velocity fluctuation, w_{rms}, is $\dot{h}$. Physically, this scaling expresses that, in that region, thermals sink at a velocity comparable to the rate of deepening.

Assuming that heat transfers between thermals and anti-thermals are controlled by molecular diffusion in the entrainment layer, one can write

$$\frac{\dot{h}}{d}\,\Delta T = \frac{\nu \Delta T}{d^2} \tag{A3}$$

where d is the thickness of the layer, ΔT, the scale for the temperature difference between thermals and anti-thermals, and ν, the molecular heat diffusivity ($\nu = 1.4 \times 10^{-7}$ m^2 s^{-1}, for water at 15 °C). From the above equation it appears that the layer thickness is:

$$d = \frac{\nu}{\dot{h}}. \tag{A4}$$

For typical oceanic values, $\dot{h}$ is of the order of 10^{-4} ms^{-1}, and, therefore, d is of the order of a millimeter.

In conclusion, the entrainment layer, where thermals are converted to anti-thermals by molecular diffusion, is a very thin layer and is not capable of controlling the evolution of the overall mixing processes.

15. Appendix B

Long's arguments for the interfacial layer

Long (1978) has studied entrainment in the interfacial layer (called thermocline in the present paper) between a stably stratified fluid and a turbulent convective layer. The interfacial layer is viewed as a thin layer, distinguishable from the mixed layer and occupied by wavelike motions which break and generate intermittent turbulence. Long's theoretical considerations are based on a series of arguments and global constraints on the system. The crucial parameter is the frictional Richardson number, Ri, as defined by (64). The results are expressions, in terms of powers of Ri, for the buoyancy and velocity rms fluctuations, interfacial-layer thickness, buoyancy flux and turbulence intermittency. In his paper, Long examined the case of turbulence generation at the surface by an oscillating grid. The purpose of this appendix is to apply Long's arguments to the present case of turbulence generation by a surface energy flux mu_*^3, and it is shown that the results of this analysis are entirely consistent with the solution presented in this paper.

Argument I: The buoyancy flux in the interfacial layer is due exclusively to turbulent motions, i.e.,

$$q \sim w_{\text{rms}}\, b_{\text{rms}}\, I \tag{B1}$$

where q is the buoyancy flux (the heat flux multiplied by αg), w_{rms} the rms vertical velocity, b_{rms} the rms buoyancy (the rms temperature multiplied by αg) and I the turbulence intermittency. The symbol $\sim$ means that both sides of this sign have the same asymptotic behavior in the limit as $Ri \to \infty$.

Argument II: Turbulence and waves in the interfacial layer are strongly influenced by buoyancy effects, so that kinetic energy and available potential energy are of the same order not only in the turbulent patches but also in wavelike motions:

$$w_{\text{rms}}^2 \sim \delta_3\, b_{\text{rms}} \tag{B2}$$

$$w_{\text{rms}}^2 \sim \delta_3^2\, \Delta b / h \tag{B3}$$

where δ_3 is the size of turbulent patches in the layer, and Δb the buoyancy difference across the interfacial layer ($N^2 h/2$ in this case).

Argument III: Conservation of turbulent kinetic energy requires that the energy flux at the edge of the interfacial layer be equal to the integrated buoyancy flux across the layer, i.e.,

$$w_{\text{rms}}^3 \sim q\delta \tag{B4}$$

where δ is the interfacial-layer thickness.

Argument IV: The eddies at the base of the mixed layer which contribute most to the turbulent fluctuations are in the inertial subrange, i.e.,

$$w_{\rm rms}^3 \sim \delta_3 u_*^3/h \tag{B5}$$

since the dissipation rate in the turbulent cascade is of the order u_*^3/h, and the disturbances are of the same order as δ_3, the turbulent-patch size.

This list of arguments is followed by two independent constraints intrinsic to the system. Firstly, the buoyancy flux in the interfacial layer is related to the rate of entrainment by:

$$q \sim \dot{h}\Delta b \tag{B6}$$

and, secondly, the global energy budget of the system requires that the rate of increase of potential energy is equal to the rate of input of turbulent kinetic energy at the surface, as expressed by (97):

$$h\dot{h}\Delta b \sim u_*^3. \tag{B7}$$

Instead of using this last argument, Long (1978) invokes experimental observation to show that δ is proportional to h, the mixed-layer depth, in the case of turbulence generation by an oscillating grid.

From (B1) to (B6) and $\delta \sim h$, Long concludes that:

$$q \sim u_* \Delta b\, Ri^{-7/4}, \quad w_{\rm rms} \sim u_* Ri^{-1/4},$$
$$b_{\rm rms} \sim \Delta b\, Ri^{-3/4}, \quad h \sim u_* Ri^{-7/4},$$
$$I \sim Ri^{-3/4}, \quad \delta \sim h, \quad \delta_3 \sim h Ri^{-3/4}.$$

In the present case, from (B1) to (B7), one concludes that:

$$q \sim u_* \Delta b\, Ri^{-1}, \quad w_{\rm rms} \sim u_* Ri^{-1/4},$$
$$b_{\rm rms} \sim \Delta b\, Ri^{-3/4}, \quad h \sim u_* Ri^{-1}, \quad I \sim 1,$$
$$\delta \sim h Ri^{-3/4}, \quad \delta_3 \sim h Ri^{-3/4}.$$

These last results are entirely consistent with (102) and (103). Moreover, it is worth noting that, in both cases, $I \sim \delta_3/\delta$, which is internally consistent with the definition of intermittency in the interfacial layer as the ratio of the volume occupied by turbulent patches to the volume of the layer. This definition could have been stated *a priori* as an alternate argument in replacement of any other (independent) argument. The result that the turbulence intermittency is of the order of unity for the present application is entirely compatible with the concept of a two-fluid system, i.e., that the flow is either downward or upward but always contributes to turbulent fluxes.

16. Acknowledgements

The author gratefully wishes to acknowledge Dr James J. O'Brien for thesis support and encouragement throughout this research. Thanks are extended to Drs Albert Barcilon, Pearn Niiler and Steven Piacsek, with whom the author had fruitful discussions, and to Drs Sergei Kitaigorodskii and Rory Thompson for a careful and constructive review of the manuscript. This work was supported by ONR Grant No. N00014-80-C-0076 and constitutes contribution No. 168 of the Geophysical Fluid Dynamics Institute, Florida State University, U.S.A.

REFERENCES

Cushman-Roisin, B. 1981. A general theory of convection: modelling by two buoyant interacting fluids. *Geophys. Astrophys. Fluid Dyn.*, in press.

Denman, K. L. 1973. A time-dependent model of the upper ocean. *J. Phys. Oceanogr. 3*, 173–184.

Denman, K. L. and Miyake, M. 1973. Upper layer modification at Ocean Station *Papa*: Observations and simulation. *J. Phys. Oceanogr. 3*, 185–196.

de Szoeke, R. A. and Rhines, P. B. 1976. Asymptotic regimes in mixed-layer deepening. *J. Mar. Res. 34*, 111–116.

Dillon, T. M. and Powell, T. M. 1979. Observations of a surface mixed layer. *Deep-Sea Res. 26A*, 915–932.

Garwood, R. W., Jr. 1977. An oceanic mixed layer model capable of simulating cyclic states. *J. Phys. Oceanogr. 7*, 455–468.

Halpern, D. 1974. Observations of the deepening of the wind-mixed layer in the northeast Pacific Ocean. *J. Phys. Oceanogr. 4*, 454–466.

Kantha, L. H., Phillips, O. M. and Azad, R. S. 1977. On turbulent entrainment at a stable interface. *J. Fluid Mech. 79*, 753–768.

Kantha, L. H. 1980. Experimental simulation of the 'retreat' of the seasonal thermocline by surface heating. *Fjord Oceanography*, Freeland, Farmer and Levings, eds., Plenum Publishing Corp., 197–204.

Kato, H. and Phillips, O. M. 1969. On the penetration of a turbulent layer into a stratified fluid. *J. Fluid Mech. 37*, 643–665.

Kim, J. W. 1976. A generalized bulk model of the oceanic mixed layer. *J. Phys. Oceanogr. 6*, 686–695.

Kitaigorodskii, S. A. 1979. Review of the theories of wind-mixed layer deepening. *Marine Forecasting*, Nihoul, ed., Elsevier Oceanography Series *25*, 1–33.

Kitaigorodskii, S. A. 1981. On the theory of the surface-stress induced entrainment at a buoyancy interface (toward interpretation of KP and KPA experiments). *Tellus 33*, 89–101.

Klein, J. P. 1980. Modélisation des méchanismes turbulents dans les couches marines superficielles. Thèse de doctorat d'Etat, Université d'Aix, Marseille II France, 167 pp.

Kraus, E. B. and Turner, J. S. 1967. A one-dimensional model of the seasonal thermocline. II. The general theory and its consequences. *Tellus 19*, 98–105.

Kullenberg, G. 1977. Entrainment velocity in natural stratified vertical shear flow. *Estuarine and Coastal Mar. Sci. 5*, 329–338.

Kundu, P. K. 1980. A numerical investigation of mixed-layer dynamics. *J. Phys. Oceanogr. 10*, 220–236.

Kundu, P. K. 1981. Self-similarity in stress-driven entrainment experiments. *J. Geophys. Res.* in press.

Linden, P. F. 1975. The deepening of a mixed layer in a stratified fluid. *J. Fluid Mech. 71*, 385–405.

Long, R. R. 1978. The growth of the mixed layer in a turbulent stably stratified fluid. *Geophys. Astrophys. Fluid Dyn. 11*, 1–12.

Manins, P. C. 1977. Fumigation and a laboratory experiment. *Weather 32*, 221–228.

Mellor, G. and Durbin, P. A. 1975. The structure and dynamics of the ocean surface mixed layer. *J. Phys. Oceanogr. 5*, 718–728.

Moore, M. J. and Long, R. R. 1971. An experimental investigation of turbulent stratified shearing flow. *J. Fluid Mech. 49*, 635–655.

Niiler, P. P. 1975. Deepening of the wind-mixed layer. *J. Mar. Res. 33*, 405–422.

Niiler, P. P. 1977. One-dimensional models of the seasonal thermocline, *The sea*, Vol. *6*, *Marine Modeling*, Goldberg et al., eds., Wiley, 97–115.

Niiler, P. P. and Kraus, E. B. 1977. One-dimensional models of the upper ocean. *Modelling and Prediction of the Upper Layers of the Ocean*, E. B. Kraus, ed., Pergamon Press, 143–172.

Piacsek, S. A. 1968. Numerical experiments on convective flows in geophysical fluid systems, *Proc. Seventh Symp. on Naval Hydrodynamics*, Rome, Italy, 753–783.

Pollard, R. T., Rhines, P. B. and Thompson, R. O. R. Y. 1973. The deepening of the wind-mixed layer. *Geophys. Fluid Dyn. 4*, 381–404.

Price, J. F. 1979. On the scaling of stress-driven entrainment experiments. *J. Fluid Mech. 90*, 509–529.

Price, J. F., Mooers, C. N. K. and Van Leer, J. C. 1978. Observation and simulation of storm-induced mixed-layer deepening. *J. Phys. Oceanogr. 8*, 582–599.

Turner, J. S. 1969. A note on wind mixing at the seasonal thermocline. *Deep-Sea Res.* Suppl. Vol. *16*, 297–300.

Turner, J. S. 1973. *Buoyancy Effects in Fluids*, Cambridge Univ. Press, 367 pp.

Turner, J. S. and Kraus, E. B. 1967. A one-dimensional model of the seasonal thermocline. I. A laboratory experiment and its application. *Tellus 19*, 88–97.

Warn-Varnas, A. C. and Piacsek, S. A. 1979. An investigation of the importance of third-order correlations and choice of length scale in mixed layer modelling. *Geophys. Astrophys. Fluid Dyn. 13*, 225–243.

Zilitinkevich, S. S., Chalikov, D. V. and Resnyansky, Y. D. 1979. Modelling the oceanic upper layer, *Oceanol. Acta 2*, 2, 219–240.

УГЛУБЛЕНИЕ СЛОЯ ВЕТРОВОГО ПЕРЕМЕШИВАНИЯ: МОДЕЛЬ ВЕРТИКАЛЬНОЙ СТРУКТУРЫ

Новая нелинейная модель перемешивания и конвекции, основанная на моделировании двух взаимодействующих жидкостей с плавучестью, применяется к описанию углубления слоя ветрового перемешивания. Ввиду простых алгебраических соотношений модель одномерна, не обладает трением и в ней пренебрегается производством турбулентности сдвигом среднего потока в термоклине. Увеличение потенциальной энергии, требуемое для углубления, поставляется при этом вводом турбулентности на поверхности (турбулентная эрозионная модель). В случае хорошо перемешанного слоя, ограниченного снизу резким термоклином, трактуемым как пограничный слой, найдено неавтомодельное аналитическое решение. Это решение справедливо, если фрикционное число Ричардсона Ri, определенное как отношение полной плавучести перемешанного слоя к квадрату скорости трения, много больше единицы. Модель предсказывает скорость вовлечения, пропорциональную R_i^{-1}, и отношение толщины термоклина к глубине слоя перемешивания порядка $R_i^{-3/4}$. Термоклин утоньшается как $h^{-1/2}$ по мере того, как глубина слоя перемешивания h растет со временем. Решение дает вертикальную структуру в слое перемешивания и в термоклине и на этой основе представлены вертикальные профили средних величин и вертикальных потоков. Эти профили сравниваются с таковыми, полученными в численных моделях с замыканием уравнений для турбулентности.